

XMM-Newton CCF Release Note

XMM-CCF-REL-266

Refinement of pn redistribution

F. Haberl, R. Saxton, M. Guainazzi, M. Stuhlinger

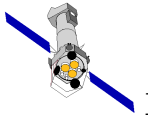
June 17, 2010

1 CCF components

Name of CCF	VALDATE	List of Blocks changed	Change in CAL HB
EPN_REDIST_0011	2000-01-01T00:00:00	NOISE_PARAM	NO
EPN_REDIST_0011	2000-01-01T00:00:00	PARTEVENT_PARAM	NO

2 Changes

The main change in the redistribution matrix of the EPIC-pn camera was a refinement of the energy resolution parameters over the whole energy band. For energies below 2 keV emission line rich spectra, mainly from the SNR 1E0102.2-7219 and the star ζ Puppis, were used for the recalibration. The input spectral models were derived using RGS spectra (see, *e.g.*, Plucinsky et al. 2008 for 1E0102.2-7219). The available pn spectra of 1E0102.2-7219 and ζ Puppis allowed direct calibration of the energy resolution for full frame (FF), small window (SW) and large window mode (LW). The parameters for all other modes were extrapolated from the full frame mode. For energies around 6 keV the Mn K_{α} produced by the on-board calibration source was used. Due to the slight decrease of charge transfer efficiency with time, the energy resolution was adjusted to yield a zero line width for the beginning of the mission. Again, this was calibrated on full frame mode spectra and extrapolated for other readout modes assuming the same energy dependence of the energy resolution. Further adjustments were done on the re-distribution caused by partial events at energies below ~ 500 eV to better fit the low-energy N-lines of ζ Puppis and to fit the spectrum of the neutron star RX J185635-3754 (assuming an absorbed blackbody spectrum). The re-distribution parameters are assumed to be mode independent.



3 Estimated scientific quality

This EPIC-pn redistribution CCF update will have a global impact on the spectral modelling of line-rich as well as continuum sources.

Line profiles are expected to be better described by redistribution matrices generated with the new CCF constituent. In Fig. 1 we show a few representative examples of improvements in the quality of the spectral fits on:

- the SNR 1E0102.2-7219. As mentioned in Sect. 1, an empirical model for this source was defined using its cumulative RGS spectrum, which is regularly measured alongside the EPIC ones in the framework of the XMM-Newton Routine Calibration Plan (RCP). This source exhibits prominent and well isolated emission lines of OVII, OVIII, NeIX, and NeX. The model was applied to the EPIC-pn spectra in the 0.15-2 keV energy band only (see Plucinsky et al. 2008 for more details). In Fig. 1 we compare the results of spectral fits performed with a matrix calculated with the public (*left column*) and the new EPN_REDIST_0011 redistribution CCF (*right column*) for observations in LW and SW. The improvement is evident from the direct comparison between the line profile in the data and in the model as well as from a significant improvement in the quality of the fit (decrease of the χ^2 ; compare the 1a f in the QDP plots of Fig. 1)
- the star ζ Puppis. Also in this case an empirical model (still unpublished) was defined on the basis of the cumulative RGS spectrum of this source, which belongs to the RCP as well. In Fig. 1 we compare the results of the application of matrices generated with the public (*left column*) and the new EPN_REDIST_0011 CCF (*right column*). ζ Puppis has a somewhat complementary soft X-ray spectrum to that of 1E0102.2-7219, due to its strong Nitrogen emission lines around 400 eV. We stress in particular the better agreement with the new calibration in the 0.15–0.3 keV energy range due to the more accurate modelling of redistributed photons from these lines.
- the highly obscured nearby Seyfert galaxy Circinus Galaxy. Its high-energy continuum ($E > 4$ keV) is dominated by Compton-reflection of the AGN primary emission, as well as by strong fluorescent lines of Fe K_α and K_β , and Ni K_α (Molendi et al. 2003). High-resolution spectra with the *Chandra* HETG unveiled the presence of a Compton-shoulder of the Fe K_α line (Bianchi et al. 2002), with an intensity close to the maximum value allowed by simulations (Matt 2002). The plots in Fig. 1 show the residuals against a best-fit model including all these physically motivated components once the intrinsic width of the line is constrained to be 0, as expected for a reprocessing system at very large distance from the black hole. The profile in a redistribution matrix calculated with EPN_REDIST_0011 follows much better the observed line shape, as well as matching more accurately the line intensity peaks.

The plots in Fig. 1 are intended as simple illustration of the changes in the quality of the spectral fits. A systematic study evaluating on a statistical basis the improvements in the quality of spectral fitting with the new CCF is deferred to Sect. 4.

Because CCF EPN_REDIST_0011 is a new global solution of the EPIC-pn redistribution, fits based on response files calculated with such a CCF component will yield globally different solutions. In

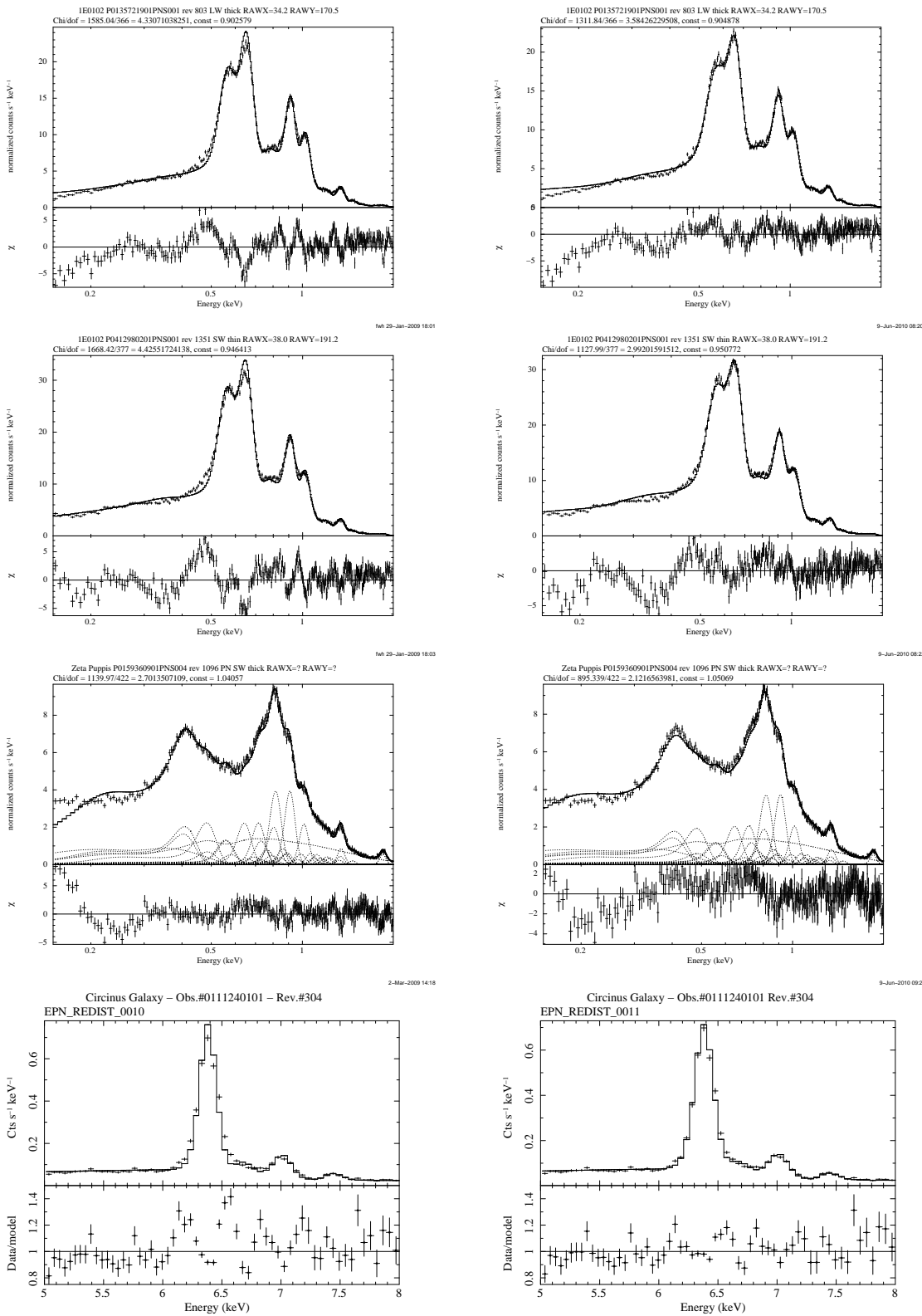
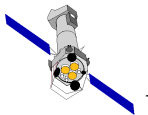


Figure 1: Spectra (*upper panels*) and residuals (*lower panels*) in units of standard deviations (1E0102.2-7219 and ζ Puppis) and data/model ratio (the Circinus Galaxy) when fits with response matrices generated with the public CCF (*left*) and with the new EPN_REDIST_0011 CCF (*right*) are performed. *From top to bottom*: 1E0102.2-7219 (LW, Obs.#0135721901), 1E0102.2-7219 (SW, Obs.#0412980201), ζ Puppis (SW, Obs.#0412980201), and the Circinus Galaxy (FF, Obs.#0111240101). Details on each source and relevant model are in text.

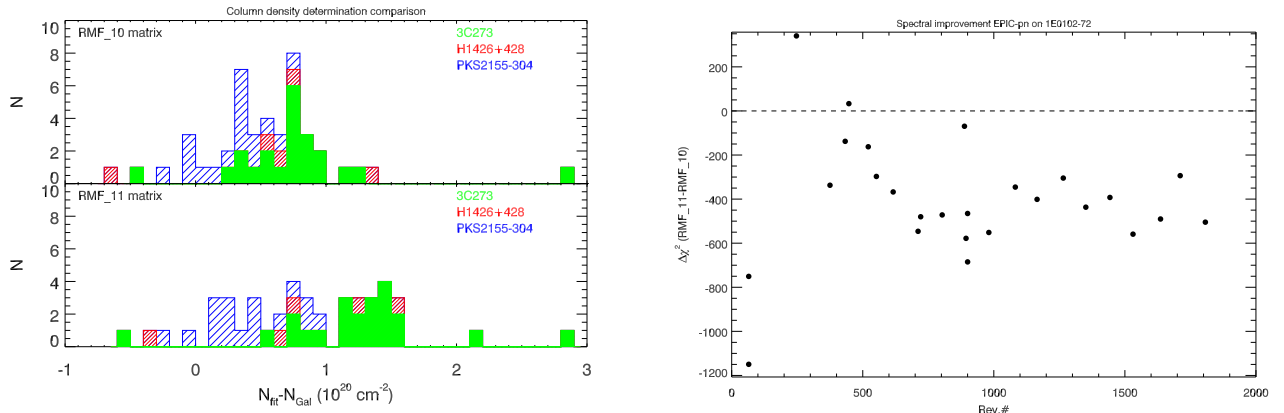
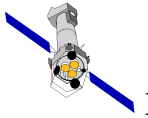


Figure 2: *Left panel:* comparison between the photoelectric absorption column densities measured with EPN_REDIST_0010 (*upper*) and EPN_REDIST_0011 (*lower*) in a sample of blazars. *Right panel:* spectral quality difference (in units of $\Delta\chi^2$) when the model defined as in Plucinsky et al. (2008) is applied to the EPIC-pn spectra of 1E0102.2-7219 with response matrices calculated with EPN_REDIST_0011 and EPN_REDIST_0010 as a function of time (in units of XMM-Newton orbit).

order for users to gauge the effect of this change, we show in Fig. 2 a comparison of the column density N_H (normalised to the contribution due to the Galaxy) along the line-of-sight to a sample of blazars, routinely observed by XMM-Newton in the framework of its routine calibration program. The average N_H difference is $\simeq 1 \times 10^{20} \text{ cm}^{-2}$ in 3C273, and $\leq 1 \times 10^{20} \text{ cm}^{-2}$ in PKS2155-304 and H1426+428. An opposite effect is shown in Fig. 3 for the super-soft spectrum of the neutron star RX J185635-3754. The average column density (measured assumed a photoelectrically absorbed single-temperature blackbody emission; see Burwitz et al. 2003 for a more detailed astrophysical discussion) decreases by $\simeq 2 \times 10^{19} \text{ cm}^{-2}$, while the average temperature decreases by $\simeq 1.5 \text{ eV}$.

Last, but not least, the new EPIC-pn redistribution significantly improve the cross-calibration between EPIC-pn and RGS below $\simeq 0.5 \text{ keV}$. The cross-calibration uncertainties are now within $\pm 3\%$ (Stuhlinger et al., 2008; Pollock & Gonzalez-Riestra 2010).

4 Test procedure and results

Systematic tests on large sample of observations of different calibration and astrophysical sources have been performed to assess the quality of the spectral deconvolution with the new CCF. We summarise here the results on the whole sample of observations of the SNR 1E0102.2-7219 performed along the mission, as well as on the internal calibration source.

4.1 1E0102.2-7219

In the *right panel* of Fig. 2 we show the difference in χ^2 between fits of the SNR 1E0102.2-7219 EPIC-pn spectra with the new EPN_REDIST_0011 and the public CCF (*negative* values mean an

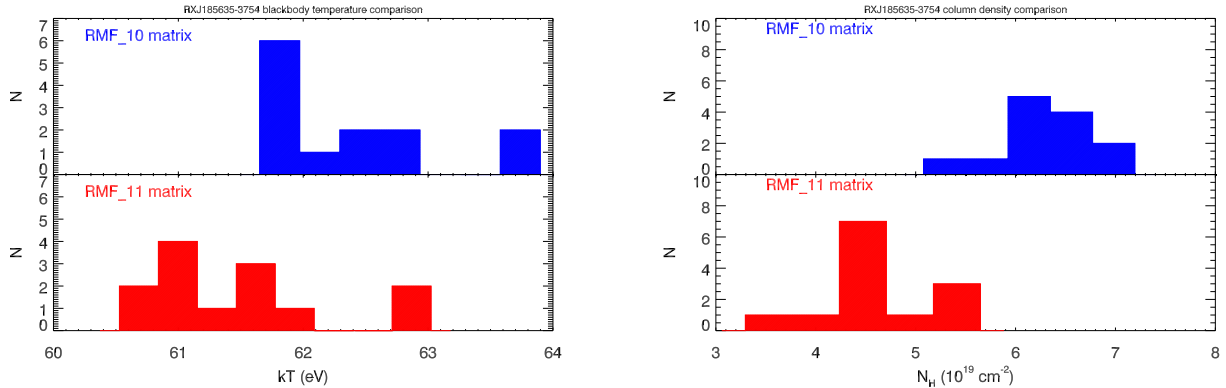
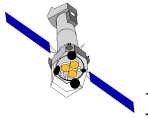


Figure 3: Comparison between the temperature (*left panel*) and column densities (*right panel*) measured from the super-soft spectrum of the neutron star RX J185635-3754 when a fit with a single-temperature photoelectrically absorbed blackbody is performed using matrices generated with the public redistribution CCF (*upper panel*) and with EPN_REDIST_0011 (*lower panel*).

improvement in the quality of the fit with the new calibrations). The $\Delta\chi^2$ values refer to fit on the whole 0.3–10 keV energy band with the model defined as in Plucinsky et al. (2008). The number of corresponding degrees of freedom is comprised between 300 and 400. In 27 out of $\simeq 30$ observations $\Delta\chi^2 < -100$, and only in 1 observation one observes a worsening of the fit quality.

4.2 Calibration source

In Fig. 4 we compare the width ($1-\sigma$) as measured by a fit with a one or two Gaussian profile of the Mn $K\alpha$ calibration line as a function of time (in units of satellite revolution) when the public (*left panel*) and the EPN_REDIST_0011 redistribution CCF (*right panel*) are used. In the latter case the width at the beginning of the mission is consistent with zero, as expected. The increasing width of the calibration line with time is a known effect. It indicates a possible worsening of the instrumental resolution with time due to a decrease of the charge transfer efficiency. It is not currently corrected in the SAS. However, analysis of several independent astrophysical sources (η Carinae, highly obscured AGN; still unpublished) does not confirm this result, and suggests instead a constant resolution (at a level consistent with the values measured as of Rev.#1200). Investigation is ongoing to assess the nature of this discrepancy.

5 Expected Updates

Investigation is being undertaken on the possibility of including a time-dependency of the energy resolution, as well as a mode-dependency of the redistribution.

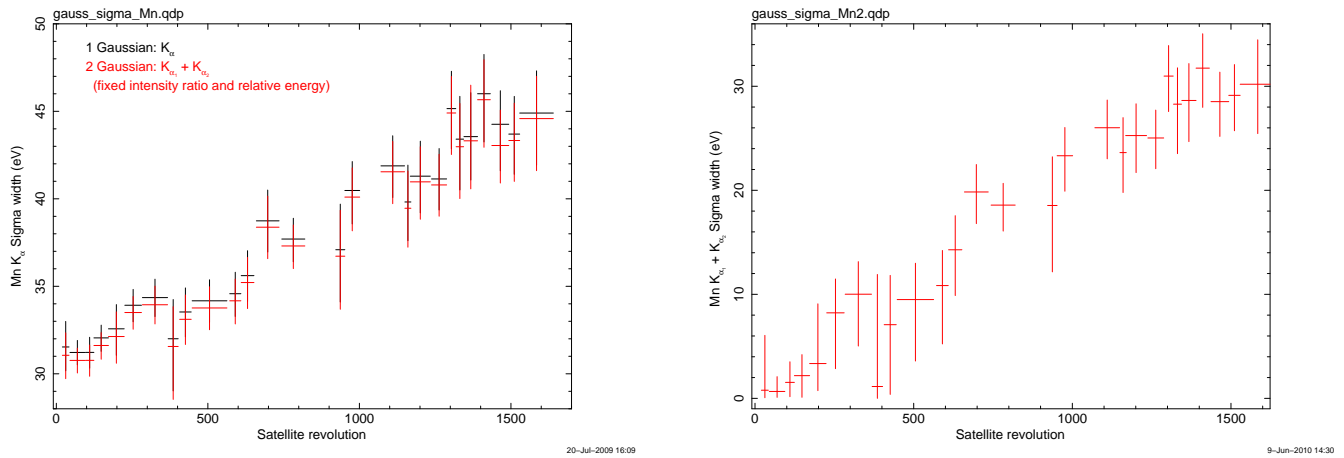
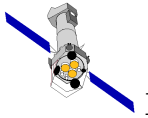


Figure 4: Comparison between the width of a Gaussian fit of the Mn K_{α} calibration line as a function of time (in units of satellite revolutions). The width of the σ parameter of a Gaussian profile in XSPEC. *Black* points indicate a fit with a single Gaussian; *red points* with a double Gaussian, taking into account the doublet nature of the Mn K_{α} transition, with the energy difference between the doublet components held fixed to the value dictated by the atomic physics.

References

Bianchi S., et al., 2002, A&A, 396, 793

Burwitz et al., 2003, A&A, 399, 1109

Matt G., 2002, MNRAS, 337, 147

Molendi S., et al., 2003, MNRAS, 343, L1

Plucinsky P., et al., 2008, SPIE, 7011, 68

Pollock A., Gonzalez-Riestra G., 2010, in preparation

Stuhlinger M., et al., 2008, "Status of XMM-Newton cross-calibration with SASv10.0", in preparation